# Technical Report SNMREC/TR-12-003

**February, 2012**

# Anchor Selection Study for Ocean Current Turbines

by

**James H. VanZwieten Jr., Michael G. Seibert, Karl von Ellenrieder**

## Southeast National Marine Renewable Energy Center

### College of Engineering and Computer Science / Florida Atlantic University

**Anchor Selection Study for Ocean Current Turbines**

by

James H. VanZwieten Jr., Michael G. Seibert, Karl von Ellenrieder

**ABSTRACT**

This paper compares anchoring systems suitable for ocean current turbines, specifically those proposed to be installed off the coast of Southeast Florida near latitude 26° 5' N. This location boasts an ocean current resource with a mean kinetic energy flux of approximately 2.34 kW/m$^2$. Bottom types ranging from unconstrained sediment to high relief ledges were observed during regional benthic surveys and therefore the performance of deadweight, plate, pile, and drag embedment anchors are compared. Numerical simulations of single point moored marine hydrokinetic devices were used to extract anchor loading at two theoretical deployment locations, mooring scopes from ranging 1.25 to 2.0, and turbine rotor diameters between 3 and 50 m. These anchor loading data were used for preliminary sizing of deadweight and driven plate anchors on both cohesionless and cohesive soils. For all evaluated scenarios, a 14 kN deadweight anchor with no shear keys is sufficient for holding a turbine with a rotor diameter of 50 m and plate anchors can also support these same loads if adequate sediment depths exist. Finally, the capabilities of drag embedment and pile anchors relevant to ocean current turbines are discussed. Multiple types of drag embedment anchors can support all of the predicted loads if adequate sediment exists and the loading is horizontal, while pile and H-type anchors can support all of the evaluated loading scenarios and chain-in-hole anchors can support turbines with rotor diameters up to 30 m.

## 1. **Introduction**

The Florida Straits located between South Florida's eastern coast and the western coasts of the Bahamian Islands is being studied with great interest because of its ocean current energy production potential. Ocean current measurements collected in this area using a subsurface ADCP buoy (26° 6.6'N, 79° 30.0'W) over a 19 month period, from May 18, 2000 through November 27, 2001, measured currents that exceeded 2.0 m/s over the upper 100 m of the water column and 1.8 m/s over the upper 200 m (Raye 2002). The mean current speeds for this 19 month deployment, recorded 3 miles west of the mean axis of the Florida Current, exceeded 1 m/s to a depth of 150 m (Driscoll et al. 2008). Maximum current velocities measured during a second 13 month ADCP deployment (26° 4.3'N, 79° 50.5'W) occurred near the surface and decrease with depth, revealing that approximately 50% of the Florida Current's available power was located in the upper 100 m (Duerr and Dhanak 2010). The mean current velocity at 50 m, a target depth for ocean current turbines, was 1.54 m/s with a standard deviation of 0.24 m/s (Raye 2002).

Ocean Current Turbines (OCT)s will require anchor systems to hold position in energy dense locations, while surviving extreme metocean conditions. Multiple hydrokinetic turbine development efforts are currently underway, with the goal of deploying commercially viable devices using single or multi-point moored systems. Two proposed single point moored designs include a dual rotor system designed for the Florida Current by Aquantis LLC (VanZwieten et al. 2006.a) and the 2nd generation contra-rotating marine current turbine developed by the Energy Systems Research Unit (ESRU) at the University of Strathclyde (Clarke et al. 2009). It was suggested by Clarke et al. (2009) that it will be necessary to deploy large machines in deep water using low cost flexible,

single riser, tensioned moorings if large scale commercial deployment is to be achieved. To operate in the strong near surface currents, significant buoyancy is designed into the nacelle ESRU's 2$^{nd}$ generation prototype system (Clarke et al. 2009). An alternative to using positive buoyancy to produce lift is seen in (VanZwieten et al. 2006.b). This design utilized lifting surfaces for variable depth operation.

To date, there have been few multi-month deployments of anchored systems in or near the Florida Current. The deployments have primarily been weather and instrumentation buoys. One such example is NOAA's 6 m long Nomad weather buoy, several of which are located off the Coast of Cape Canaveral (NDBC 2010). These buoys are smaller than, and create less drag force than is expected from full scale OCTs. No attempts have yet been made to anchor energy production facilities in the Florida Current for more than a day.

The only example of an MRE device being deployed in the Florida Current occurred in April of 1985 when Nova Energy Limited deployed a Vertical Axis Hydro Turbine from a moored ship that extracted energy from the current for less than a day (Davis et al. 1986). Difficulties during testing proved to engineers that the mooring system has a significant effect on both cost and viability of a design (Davis et al. 1986). This report suggested that the construction and setting in place of very large gravity anchors near the core of the Florida Current was the major cost item for the mooring system. Finally, this report suggested that during the costly development and deployment of prototype MRE devices, the design of the anchoring and mooring system must be given adequate attention, such that it does not hinder device feasibility.

Anchoring system studies relevant to OCT installation require a thorough investigation of the ocean current and the benthic environment. The investigation of proposed OCT designs showed that OCTs will most likely operate without a surface presence and at depths where the environmental forcing from waves is minimal. Although of great importance during system deployment and recovery, wind speeds and wave conditions were not considered in this study. Therefore, the extreme current condition is the driving factor that was used to calculate the anchor loadings; while the benthic environment directly influences the type, size, and deployment location of the anchors that can be used.

The Southeast National Marine Renewable Energy Center (SNMREC) is leading a multi-phase effort to create offshore energy testing capabilities in the Florida Current for testing in-stream hydrokinetic devices (Driscoll et al. 2008). SNMREC initially proposed a Limited Lease for Alternative Energy Resource Assessment and Technology that is located off the coast of Ft. Lauderdale, which is referred to for the remainder of this work as the "area of interest" (Figure 1). The proposed lease area has been refined, however, the initial lease area was still considered for this anchoring study as it more generally represents a characteristic area that would be considered for OCT installation.
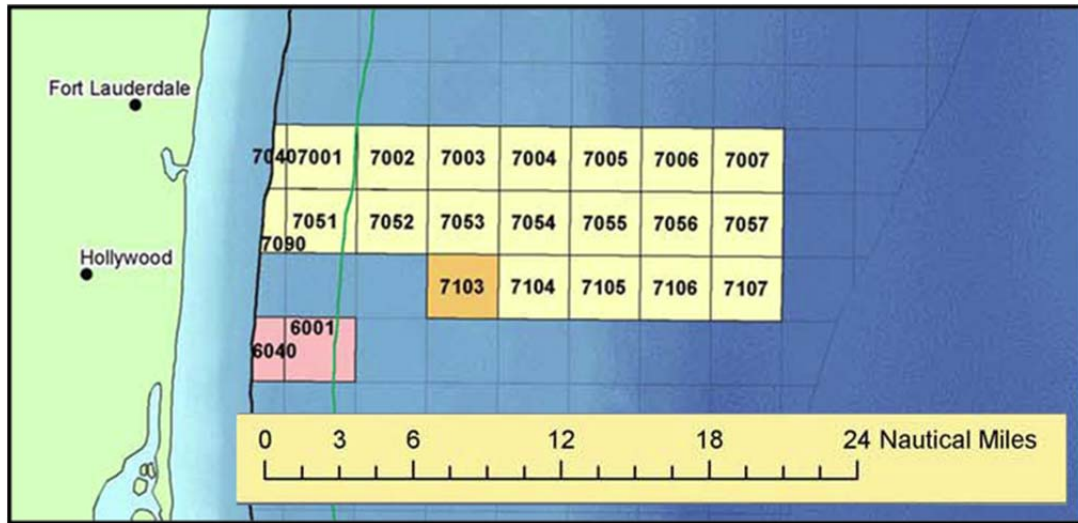
**Figure 1: FAU's initial proposed limited lease area for alternative energy resource assessment and technology development – Proposed Lease Area (in yellow). Courtesy US Dept. of Interior MMS (SNMREC, 2010).**

The focus of this work is to determine suitable anchors for mooring OCTs off the coast of Southeast Florida. Section 2 of this paper presents regionally surveyed bottom types observed in past studies and anchor types are compared for their applicability and performance for the known bottom types of the region. Section 3 explains a basis for selecting extreme ocean current conditions, which were applied to single point moored hydrokinetic turbine simulations to extract anchor loading estimates. Section 4 uses the anchor loading results from Section 3 to perform preliminary anchor sizing for single point moored marine hydrokinetic (MHK) devices for both cohesionless and cohesive soils. Finally, Section 5 discusses the results of this anchor study.

## 2. **Suitable Anchor Types**

This overview of possible anchor types for mooring OCTs in the Florida Current includes both a review of the basic applicable anchor types and the local benthic environment. The commonly used applicable anchor types are presented in Section 2.1 with relevant information on their important holding characteristics, required bottom

5

types, and primary uses. Following this, information is presented in Section 2.2 on the local benthic environment with notes on which types of anchor are likely to be applicable in the different areas.

## 2.1 Anchors

The four general anchor types evaluated in this study are deadweight (gravity), drag-embedment, pile, and plate (direct embedment) (Figure 2). Each of these anchor types has multiple design variations and deployment methods, while selection depends on both the characteristics of the seabed and direction of loading. The typical performance of these four anchor types is summarized in Table 1 for different anchoring scenarios.
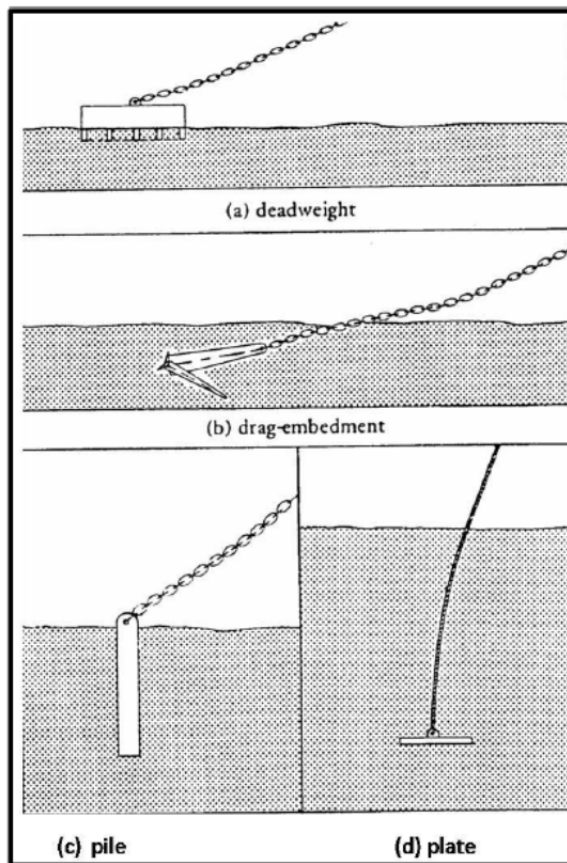


**Figure 2: "Generic anchor types" (Sound and Sea Technology 2009).**

Table 1:  Anchor behavioral criteria (Sound and Sea Technology 2009).

| *Anchor Type* | *Deadweight* | *Pile* | *Plate* | *Drag* |
|---|---|---|---|---|
| Seafloor Material | | | | |
| | | | | |
| **Soft clay, mud** | ++ | + | ++ | ++ |
| **Soft clay layer (0-20 ft) over hard layer** | ++ | ++ | O | + |
| **Stiff clay** | ++ | ++ | ++ | ++ |
| **Sand** | ++ | ++ | ++ | ++ |
| **Hard glacial till** | ++ | ++ | ++ | + |
| **Boulders** | ++ | o | O | o |
| **Soft rock or coral** | ++ | ++ | ++ | + |
| **Hard, massive rock** | ++ | + | + | o |
| | | | | |
| Seafloor Topography | | | | |
| | | | | |
| **Slope < 10 deg** | ++ | ++ | ++ | ++ |
| **Slope > 10 deg** | o | ++ | ++ | o |
| | | | | |
| Loading Direction | | | | |
| | | | | |
| **Omnidirectional** | ++ | ++ | ++ | o |
| **Unidirectional** | ++ | ++ | ++ | ++ |
| **Large uplift** | ++ | ++ | ++ | o |
| | | | | |
| Lateral Load Range | | | | |
| | | | | |
| **To 100,000 lb** | ++ | + | ++ | ++ |
| **100,000 to 1,000,000 lb** | + | ++ | + | ++ |
| **Over 1,000,000 lb** | o | ++ | O | o |

++ Functions well
+  Functions, but is normally not the best choice
o  Does not function well

## 2.2   Bottom Types and Applicable Anchors

Sources of information available on the bottom types near the area of interest include
the Final Report of the *Calypso LNG Deepwater Port Project, Florida Marine Benthic
Video Survey* (Messing et al. 2006.a), the Final Report of the *Calypso U.S. Pipeline, LLC,
Mile Post (MP) 31- MP0 Deep-water Marine Benthic Video Survey* (Messing et al.
2006.b)*,* and a set of submersible dives performed by Harbor Branch Oceanographic
Institution (HBOI) on behalf of SNMREC (SNMREC 2010). Both the Calypso port
survey and the Calypso pipeline survey occurred north of the area of interest, while the

submersible dives occurred within the area of interest. Two additional sources, Ballard and Uchupi (1971) and Neumann and Ball (1970), are geological studies of the Miami Terrace completed in the 1970s that largely appear to corroborate the findings of the three surveys mentioned above, (SNMREC 2010).

The Calypso port survey took place approximately 10 miles northeast of Port Everglades, while the Calypso pipeline survey extended from the region of the Calypso port survey and ran northeast towards Grand Bahama Island (Seibert 2011). The reports generated from these surveys list benthic habitat descriptions with accompanying longitude and latitude. Bottom types described by habitat categories of the Calypso port survey, with associated water depths between 210 and 300 m, include sediment substrates, unconsolidated mud or sand substrates (Figure 3), as well as low to high cover hard bottom (Figure 4).
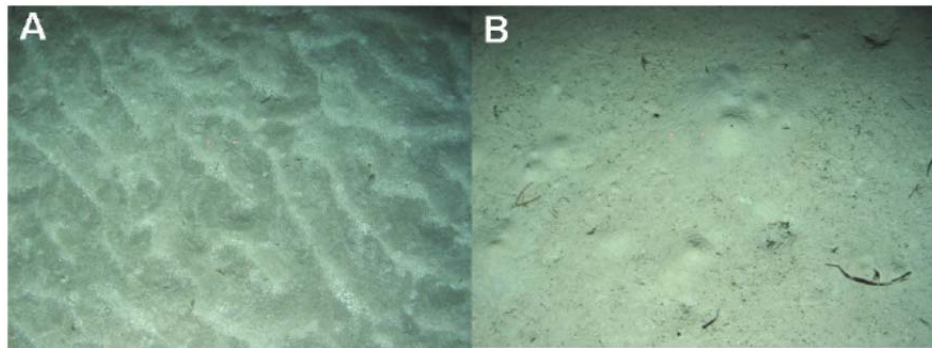


**Figure 3:  "Representative unconsolidated sediment substrates. A.  Obsolete rippled sediment, B.  Flat textured bioturbated sediment" (Messing et al. 2006.a).**
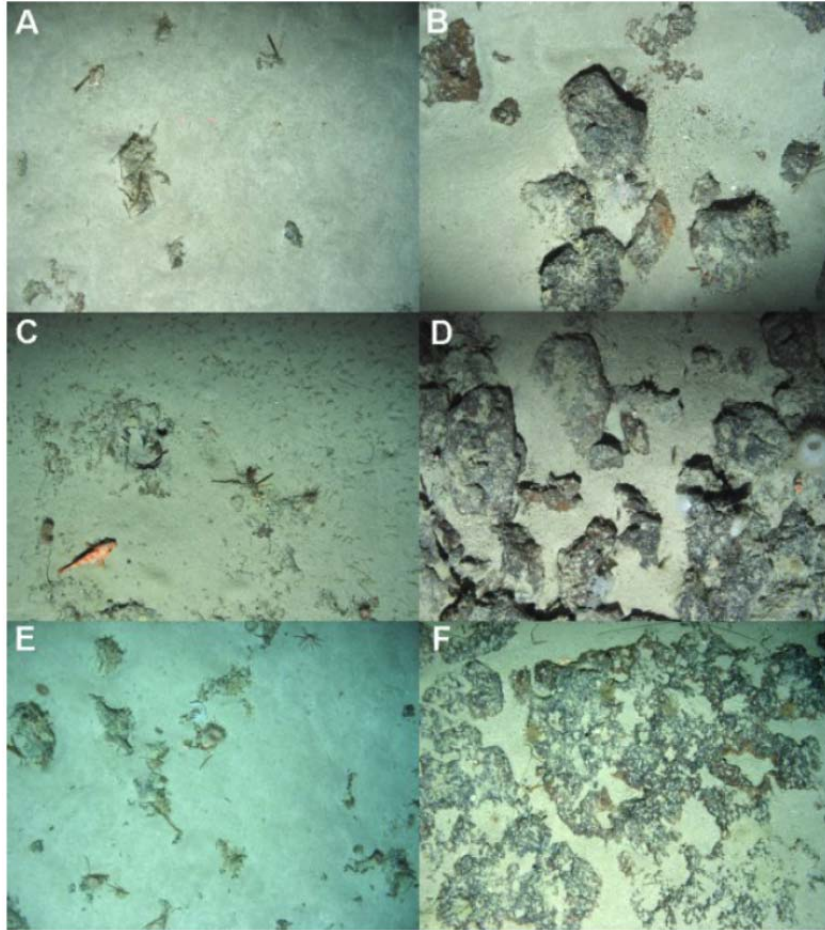
**Figure 4: "Representative low-cover (A, C, E) and high-cover (B, D, F) hard-bottom substrates" (Messing et al. 2006.a).**

Observations from the portion of the Calypso pipeline survey performed atop the Miami Terrace describe a mostly hard bottom composed of limestone slabs and pavements with different combinations of gravel, rubble, and sediment overlay (Messing et al. 2006.b). The low-relief hard bottom with some overlay changes to moderate and high relief hard bottom moving eastward down the Terrace Escarpment (Figure 5). The significant drop observed over the Terrace Escarpment is characterized by high-relief hard bottom consisting of ledges, steep slopes, and escarpments with up to 20 m relief. Beyond the Terrace Escarpment there exist regions described as alternating obsolete rippled and smooth sediment with regions of coral rubble. The associated approximate

water depths are 200 to 350 m atop the Miami Terrace, 350 to 600 m over the Terrace

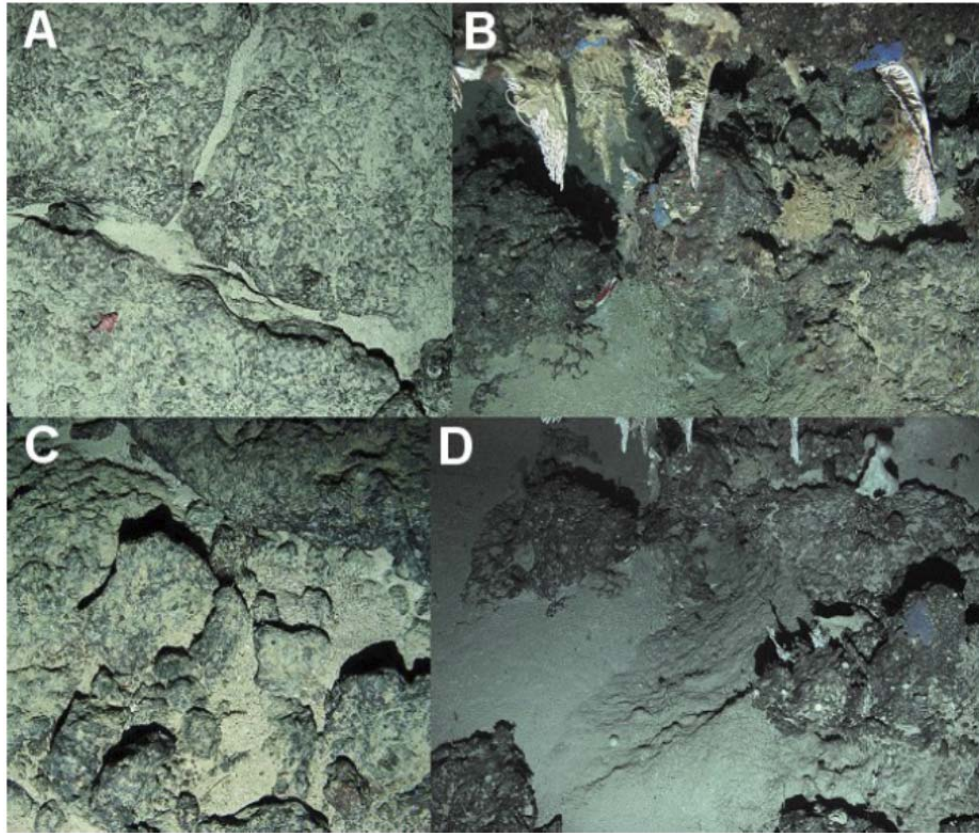Escarpment, and 600 to 800 m in the Florida Straits (Figure 6).



**Figure 5: "A. Low-relief jointed pavement on escarpment between high-relief ledges. B. Side of high-relief ledge with projecting lace corals (Stylasteridae). C. Moderate-relief outcrops and boulders. D. Steep sediment and boulder-strewn slope" (Messing et al. 2006.b).**
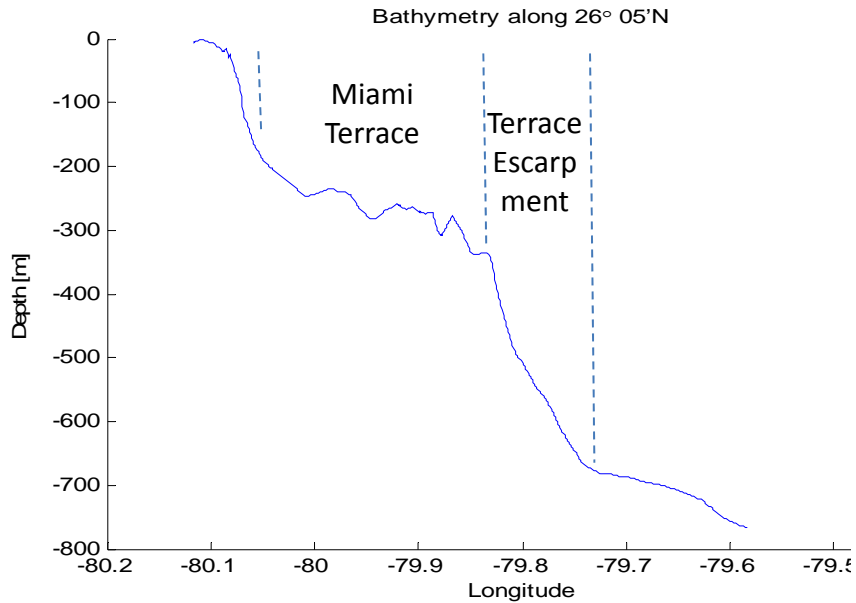
**Figure 6: Bathymetry along 26° 05'N. The estimated positions of the Miami Terrace and Terrace Escarpment at this latitude are presented.**

The two sessions of manned submersible benthic surveys that took place within the area of interest along 26°05' N (SNMREC 2010) confirmed that some sediment does collect atop the Miami Terrace and beyond the Terrace Escarpment. The full initial set of sub dive videos was recorded atop the Miami Terrace where limestone bottom overlaid by varying amounts of sediment were observed. The second set of dives recorded video and photographs of gravity anchors used to moor ADCP buoys at water depths of 260 m, 340 m, and 660 m. At 260 m, the bottom type is characterized by rubble covered by a thin sand layer, and no benthic life was found nearby. Photographs at the 340 m depth indicate sand with sparse sponge growth, but no significant coral habitat was discovered. Finally, at the 660 m site, the bottom was characterized by sand with no active benthic habitat (SNMREC 2010).

As displayed in Table 1, all four anchor types function in sand, clay or mud where adequate sediment depths exist. Only deadweight and pile anchors function well on low

to high cover hard bottom. The high relief and steep slopes that occur on the Terrace Escarpment may not be well-suited for anchoring purposes. The reasons for this are that deadweight anchors work in high relief areas, but do not function well on steep slopes. While pile or plate anchors could be examined for use on steeper slopes, these choices generally have higher design and deployment costs.

The reviewed benthic surveys provide an understanding of the bottom types that may be encountered in the selected area of interest (Figure 1). However, detailed site-specific surveys are required for final anchor system selection and design. Investigation of sediment overlay depths and soil properties necessary for anchor selection and design can be determined using sub-bottom profiling and by obtaining core samples.

### 3. **Anchor Loads**

It is expected that a commercial turbine system will require the use of adjustable buoyancy systems and/or lifting surfaces in order operate at depths selected to produce maximum energy and possibly to "dive" to a deeper depth to avoid major environmental surface forcing events such as hurricanes. Because of this avoidance expectation, wave and wind conditions were not included when calculating anchor load estimates. Water velocity profiles corresponding to maximum loading were therefore solely used for this analysis. Local current data was combined with bathymetry information along 26°5' N to develop a comprehensive range of anchor loading scenarios that may occur for future commercial MHK devices in this region. These anchor loading scenarios were simulated using Orcaflex software (Section 3.2) and the anchor loading was then extracted (Section 3.3).

## 3.1 Maximum Currents

The core of the Florida Current straddles a seafloor feature called the Terrace Escarpment, where anchoring should be avoided due to steep slopes and high relief (Figure 5). Selected anchoring scenarios are characteristic of locations both east and west of this feature. To the west of the Terrace Escarpment is the Miami Terrace with depths from 200 to 350 m and east of the Terrace Escarpment depths from 600 to near 800 m are found (Figure 6).

The maximum current data obtained from ADCP moored buoy deployments referred to in the introduction were used to simulate the maximum loading on an OCT. One set of ADCP measurements was made approximately three miles west of the mean axis of the Florida Current during 2000 and 2001, while the second set of ADCP measurements were made slightly upstream of this location during 2008 and 2009. Combining the data from the two sets of deployments provides almost three full years of current measurements in the Florida Current. Both of these data sets measured a maximum near surface current of 2.5 m/s (Raye 2002 and VanZwieten et al. 2011). The maximum current profile used for simulating an anchor loading scenario on the Miami Terrace was generated by interpolating between the maximum currents specified at depths between the surface and seafloor at 50 m increments (Figure 7). Offshore standards such as those used in the offshore oil industry recommend return periods of 10 years (DNV 2008), so continued measurements in the region may reveal even greater maximum currents that could be used for calculation. However, the load on an anchor could be significantly reduced in these extreme events by either stalling rotor blades or locating the OCT deeper in the
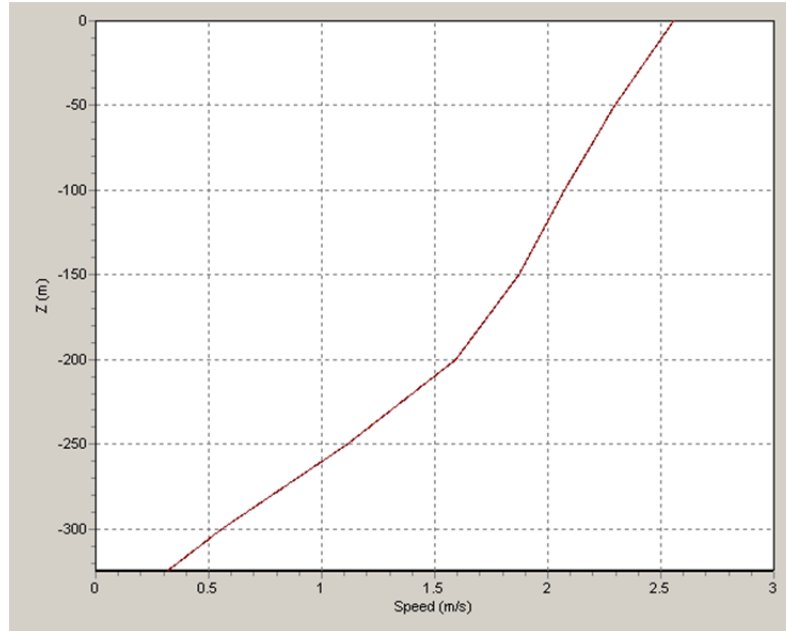
water column.



**Figure 7:  Maximum Current Profile for 325 m depth (ADCP data).**

A 700 m depth was selected to represent anchor loading scenarios east of the Terrace

Escarpment and numeric model data were used to predict maximum flow speeds. This

current profile was developed from the HYbrid Coordinate Ocean Model (HYCOM),

which is a data assimilative hybrid isopycnal-sigma-pressure (generalized) coordinate

ocean model that simulates oceanographic characteristics, including north and east

velocity values at a given location (Duerr and Dhanak 2010). The data used to create the

current profile include the maximum velocity magnitude at each depth bin for two

months of daily snapshots of the Florida Current at 27° 00' N, 79° 36' W from November

and December of 2008. The measurement location is north of the area of interest, but is

characteristic of the Florida Straits and was, until the writing of this article, the best

available estimate for the 700 m current profile that the authors possess. The resulting

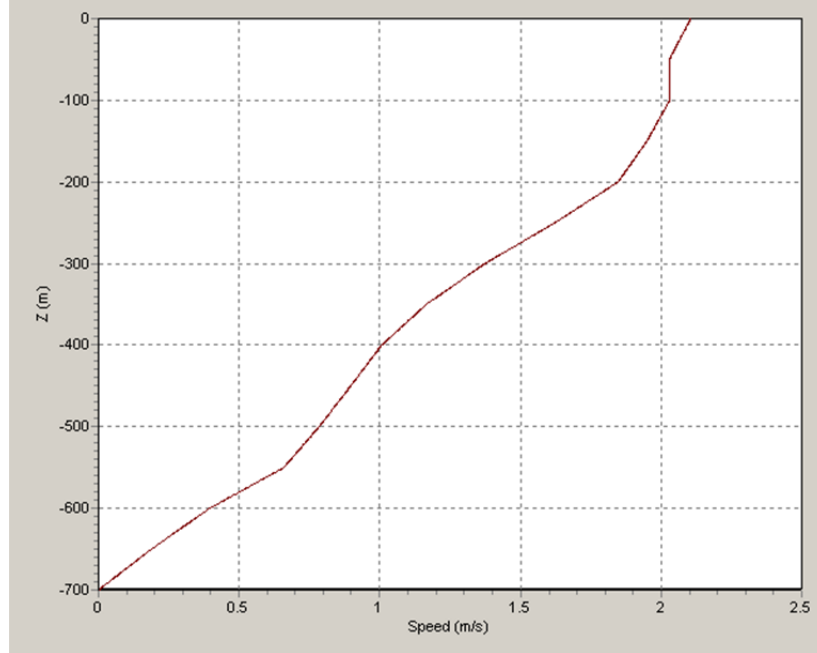current profile for the 700 m depth is displayed in Figure 8.

**Figure 8: Maximum current Profile for 700 m depth (HYCOM data).**

## 3.2  Marine Hydrokinetic Turbine Anchor Loading

In order to investigate anchoring options for in-stream hydrokinetic turbines, single point moored systems were modeled in Orcaflex using subsurface 3D buoys. The drag characteristics of these buoys were set to match the estimated drag characteristics for a turbine with the desired rotor diameter. The drag on the simulated ocean current turbine model was estimated by:

$$D = \frac{1}{2} C_d \rho U^2 A,$$  (1)

where $D$ is the drag force (commonly referred to as thrust when only the rotor is considered), $C_d$ is the drag coefficient, $\rho$ is the density of seawater, $U$ is the current speed, and $A$ is the rotor's swept area. The drag coefficient was derived from a numerical simulation developed for predicting the performance of the SNMREC experimental ocean current turbine (VanZwieten et al. 2010). This OCT design (Figure 9)

15

has a 3 m diameter rotor. The maximum drag of the SNMREC experimental OCT in a 2.5 m/s current was derived as 20.25 kN; this value includes the drag created by the generator housing, buoyancy modules, and rotor when operating with a tip speed ratio of 3.9 (which corresponds to the maximum shaft power and maximum drag). Note that rotor drag accounted for 81% of the total simulated drag, and the remaining 19% was due to the generator housing and buoyancy modules. A drag coefficient of 0.89 is then calculated for the entire turbine using (1). As expected, the drag coefficient for the rotor alone (81% of 0.89 = 0.72) is somewhat less than the value of 8/9 that Betz identifies as the drag coefficient when a rotor is operating at the maximum theoretical power coefficient (Clarke et al. 2009). A drag coefficient of 0.89 and swept area of the desired rotor size were used in the numerical simulation so that the drag on the turbine was accurately represented.
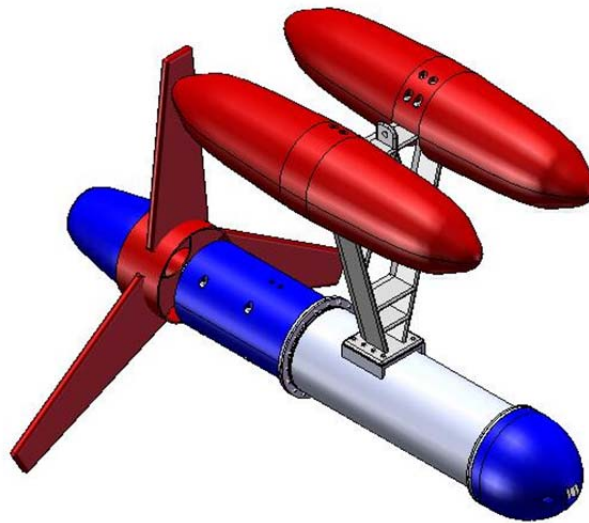


**Figure 9: CAD Drawing of SNMREC's First Generation Experimental Hydrokinetic Turbine design.**

16

For each simulation run, the mass of the turbine was set to a constant value and the buoyancy of the turbine was incremented until it reached a steady-state position within 1 m of the target operational depth of 50 m. Once operating at the target depth, the diameter of the taut mooring line (6 x 19 wire strand with wire core) was increased in increments of 0.005 m until minimum breaking loads were greater than the effective tension of the mooring line (with an applied safety factor of 2.04). As previously stated, offshore standards do not exist for this specific application, and therefore a safety factor of 2.04 was used according to DNV's *Offshore Standards for Position Moorings* (DNV 2008). The simulated moored turbine system was characterized in the class 1 consequence class, which includes position moorings "where mooring system failure is unlikely to lead to unacceptable consequences such as loss of life, collision with an adjacent platform, uncontrolled outflow of oil or gas, capsize or sinking (DNV 2008)." This selection yields a partial safety factor of 1.70 for a quasi-static analysis. The partial safety factor (applicable to chain, steel wire ropes, and synthetic fiber ropes) was then be multiplied by a factor of 1.2 to compensate for the lack of redundancy of a single point mooring, yielding a safety factor of 2.04 as suggested by (DNV 2008). When the mooring line diameter was increased, the process of varying the buoyancy of the turbine was once again repeated until the OCT remained within 1 m of the desired 50 m depth.

Multiple mooring scopes were evaluated for the two previously mentioned locations to evaluate the relationship between mooring scope and anchor loading. Scopes of 1.25, 1.5, and 2 were examined for the 325 m depth, while scopes of 1.25 and 1.5 were examined for the 700 m depth. The scopes of 1.25 and 1.5 for both simulations created an

approximate range of anchor loading angles with the seafloor from 30° to 45°, which is the loading angle range typical of taut moorings (Tension Tech 2010). A scope of 2 was applied to the 325 m depth to provide insight into the effects of larger scopes. Note that in the case of commercially deployed systems, it will be desirable to select a mooring scope large enough to allow an OCT to surface in normal operating currents for maintenance purposes. Each mooring scenario was evaluated for eight rotor diameters, ranging from 3 to 50 m.

## 3.3 Simulation Results

Forty unique mooring cases were created to define a range of anchor loading scenarios that may occur from variations in rotor size, mooring design, and location. The anchor loading and upward force required to hold turbines at a desired depth were calculated for each case.

As expected, these simulations indicate that overall anchor loading increases with decreasing scopes (Figures 10 and 11). The majority of this increase is seen in the vertical anchor loading component, which is caused by the increased buoyancy necessary for the device to remain at the same (50 m) operating depth with a shorter mooring line. For a 20 m diameter rotor operating in the 325 m water depth, the vertical loading increased from 318.5 kN, with a scope of 2.00, to 666.4 kN, with a scope of 1.25. Horizontal loads on the anchor connection point remained close to values when scopes were changed, differing by less than 5% for each rotor diameter. The same trends can be observed for the 700 m depth locations, but the overall anchor loading of the 700 m depth is less than the 325 m depth. This is due to smaller current maximums in the 700 m profile versus the 325 m

profile. A 20 m diameter rotor with a scope of 1.25 at the 325 m depth was investigated

and resulted in a line tension of 1016.6 kN at the anchor connection point, whereas at the

700 m depth scenario with the same scope was 864.9 kN of tension.
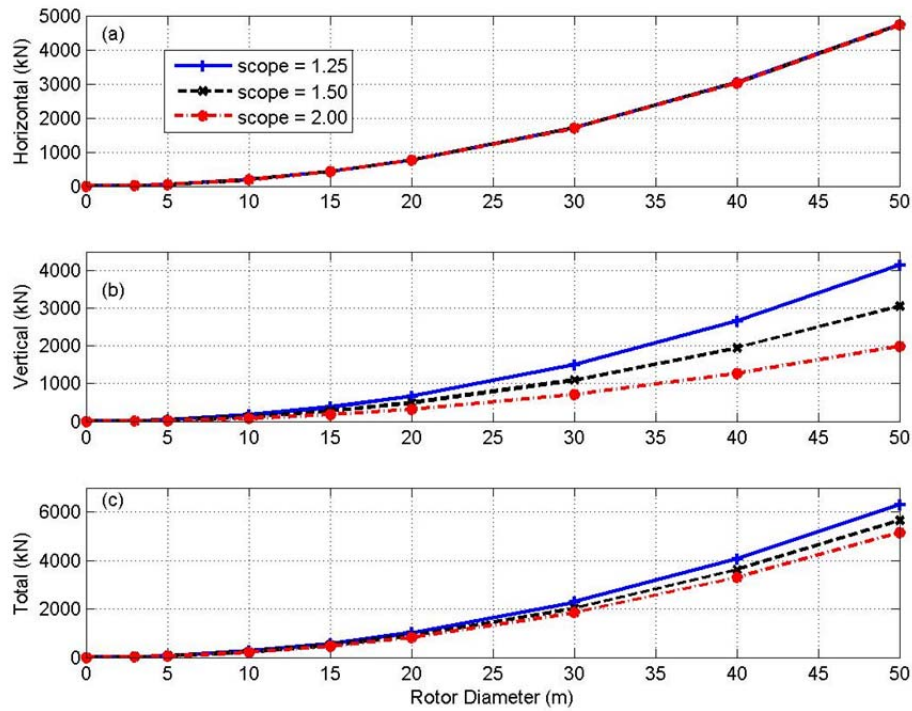


**Figure 10: Turbine anchor loading for 325 m depth. The horizontal anchor loadings (a), the vertical anchor loadings (b), and the total anchor loadings (c).**
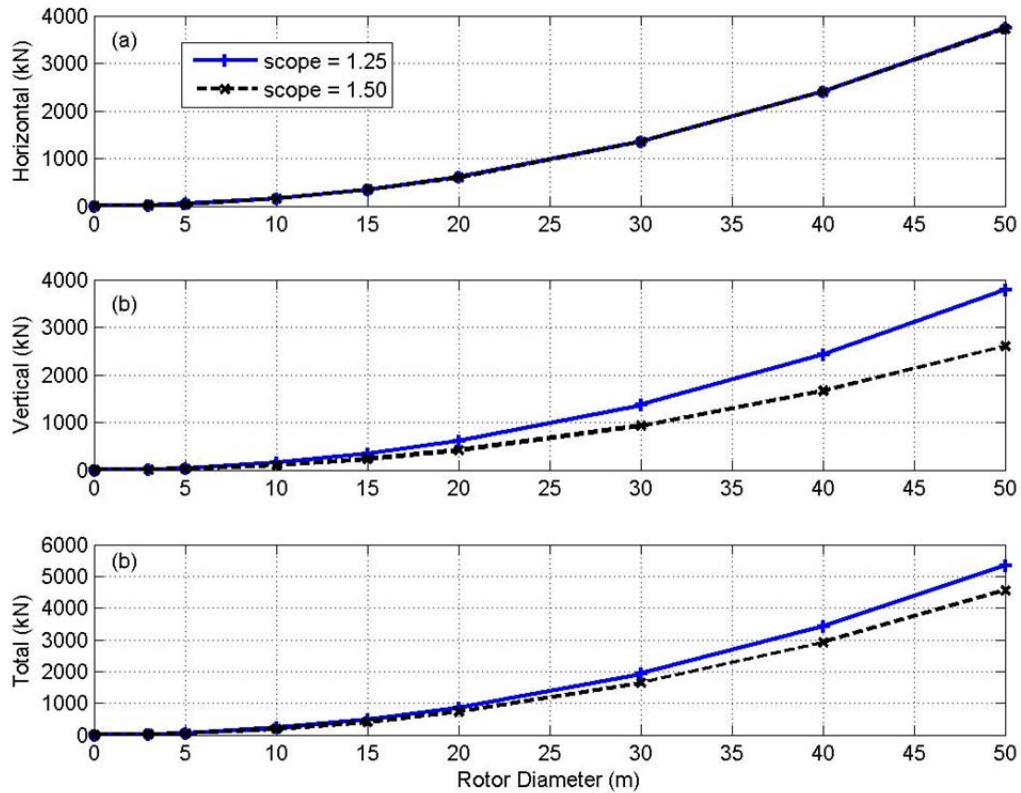
19

**Figure 11: Turbine anchor loading for 700 m depth. The horizontal anchor loadings (a), the vertical anchor loadings (b), and the total anchor loadings (c).**

The calculated lift force required to hold the simulated turbine at a depth of 50 m (Figure 12) may be useful to device developers when sizing buoyancy tanks or lifting surfaces. For an OCT with a 20 m rotor diameter operating in the 325 m velocity profile, the necessary net buoyancy force increases from 393.0 kN (for a scope of 2.00) to 727.3 kN (for a scope of 1.25). These positive buoyancies are equivalent to displacing 39.1 m$^3$ and 72.3 m$^3$ of sea water, respectively. Assuming a lift coefficient of 1.0 and no three-dimensional hydrodynamic effects, lifting areas of 145 m$^3$ and 268 m$^3$ will be required for these respective cases.
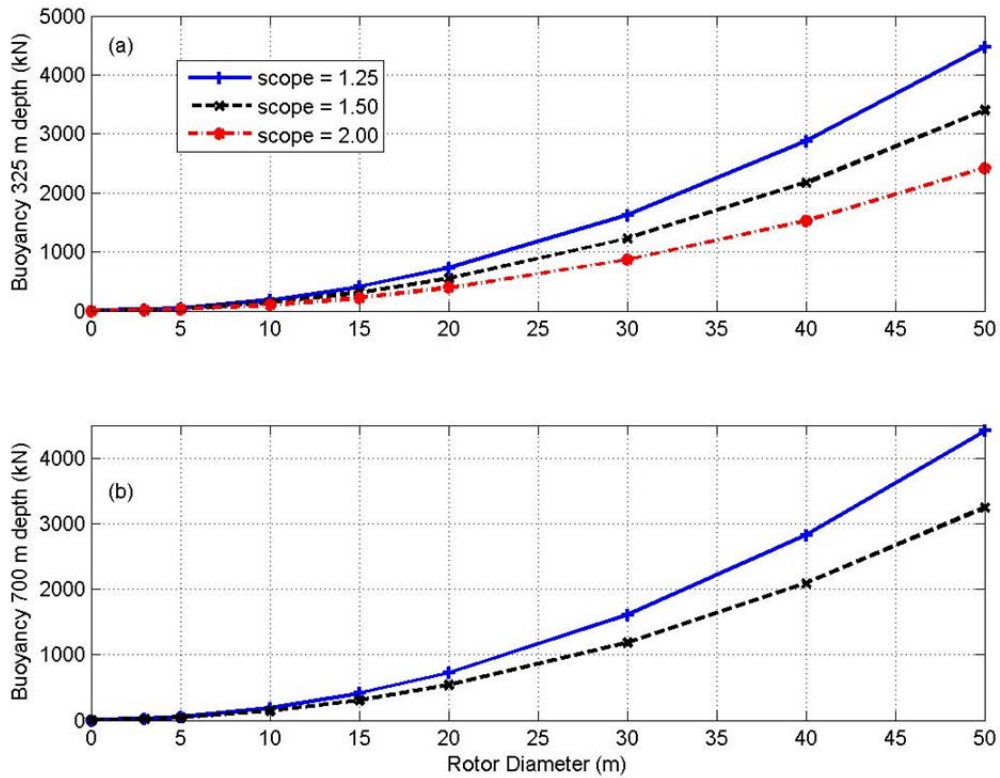
**Figure 12: Net buoyant force for turbine at a 50 m depth for the location with a 325 m depth (a) and at 700 m depth (b) locations.**

4. **Preliminary Anchor Sizing for Single Point Moored MHK Devices**

The relationship between anchor and mooring system cost and the potential power output of a specific device over its lifetime will affect the size and economic potential of commercial devices. Conceptualizing the deployment of such devices provides developers with preliminary anchor sizes and anchoring options which may impact the design of the device. Therefore, anchor sizing methods for deadweight anchors with and without shear keys, plate anchors, and drag embedment anchors were investigated. Estimates were also generated for maximum rotor diameters applicable to four common types of pile anchor. Anchor sizing estimates were determined for both cohesionless

21

(sand or gravel) and cohesive (mud, silt and clay) soil. All anchor sizing scenarios presented assumed a flat seabed.

## 4.1 Deadweight (Gravity) Anchor Sizing

Deadweight anchors can be used on each of the presented bottom types within the area of interest and require the least geotechnical data for design, making them a versatile and inexpensive option for installing an OCT on the sea floor. However, they are the least efficient of the evaluated anchor types based on their holding capacity to weight ratio. Deadweight (gravity) anchors can be selected as a commonly used design like the U.S. Navy's Pearl Harbor Anchor design (Seelig et al. 2001) or custom designed. Deadweight anchor design procedures from Navy design guides and OWET's advanced anchoring and mooring study for ocean wave energy conversion are followed in this section to provide example anchor design procedures and figures for anchor sizing reference.

### 4.1.1 Deadweight Anchor on Cohesionless Soil with no Shear Keys

The first anchor evaluated is a simple concrete sinker or squat clump-style anchor with no shear keys. The weight (in water) required to resist sliding on cohesionless soils can be calculated from:

$$W = \frac{F_h}{\tan(\phi - 5°)} + F_v, \tag{2}$$

where $F_h$ equals the horizontal anchor loading, $\phi$ is the angle of internal friction of the sediment, and $F_v$ is the vertical anchor loading (Taylor 1982). The 5° reduction in sliding friction is an average value found from empirical tests where flat anchor bottoms

22

did not cause the soil to fail by mobilizing the complete internal friction of soil (Taylor, 2010). The angle of internal friction needed for determining anchor weight on cohesionless soil can be estimated based on the soil descriptions found in (Vryhof Anchors 2005) or from on-site test-determined values. These empirically obtained values can be found using a Standard Penetration Test (SPT) or Cone Penetrometer Test (CPT) (Vryhof Anchors 2005).

After the weight (in water) required to resist sliding is determined, the minimum anchor width ($B$) without shear keys can be determined from:

$$B = \left[ \frac{6WF_h}{\gamma_s (W - F_v)} \right]^{\frac{1}{3}}, \tag{3}$$

where $W$ is the required weight in water and $\gamma_s$ is the submerged specific weight of the anchor material (Taylor 1982). The value of $\gamma_s$ for concrete is taken as 13.51 kN/m$^3$ (86 lbs/ft$^3$) as suggested by Taylor (1982). The maximum height ($H$) of the mooring line connection point above the base of the anchor can be determined as suggested by Taylor (1982),

$$H = \frac{B(W - F_v)}{6F_h}. \tag{4}$$

Finally, the length ($L$) of the anchor necessary to achieve the required weight in water can be determined by:

$$L = \frac{W}{\gamma_s HB}. \tag{5}$$

The method described was used to create Figures 13 and 14. Loose sand with an angle of internal friction of 30° is selected for the example sizing. At the 325 m location, it was

23

predicted that an OCT with a 20 m rotor diameter and mooring scope of 1.25 can be held by a concrete gravity anchor with a length, width, height, and weight of 7.8 m, 7.8 m, 2.8 m, and 2,312.8 kN respectively. This is the maximum gravity anchor size required for the evaluated 20 m diameter rotor cases. It should be noted that no safety factors other than those applied to mooring line sizing were applied to the anchor sizing calculations.
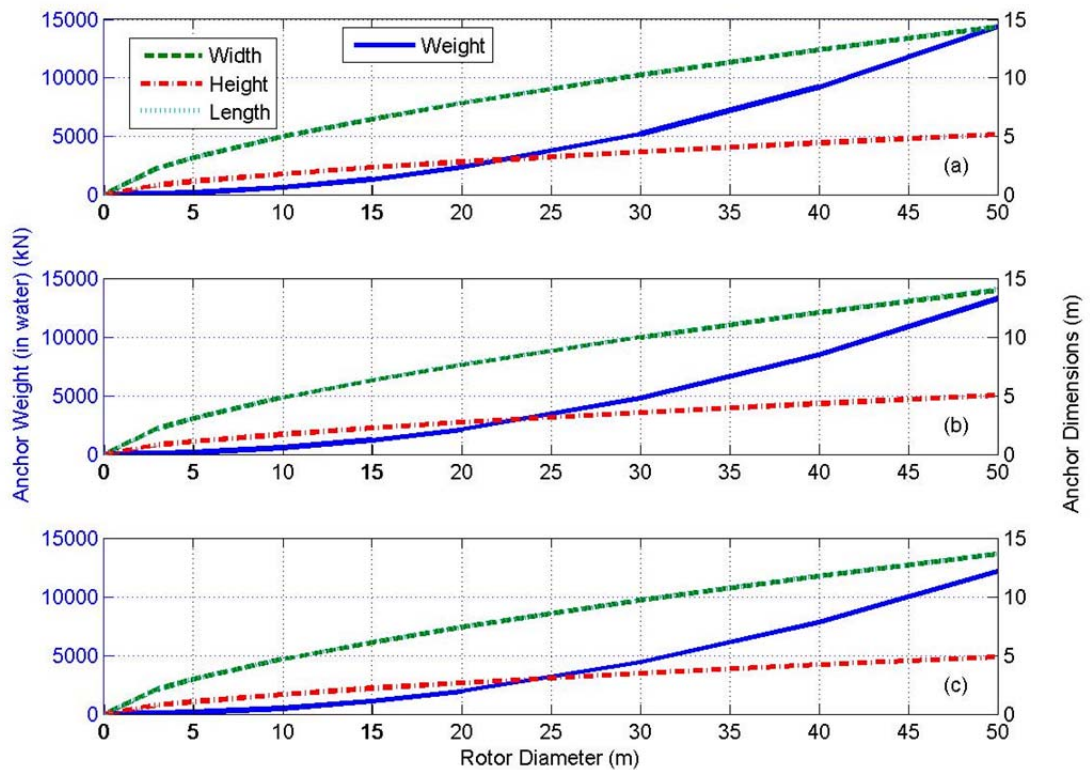


**Figure 13: Anchor dimensions for concrete deadweight anchor with no shear keys at 325 m depth location for loose sand with a friction angle of 30˚. Mooring scopes of 1.25 (a), 1.50 (b), and 2.0 (c) are presented. Anchor length and width overlay each other in this figure.**
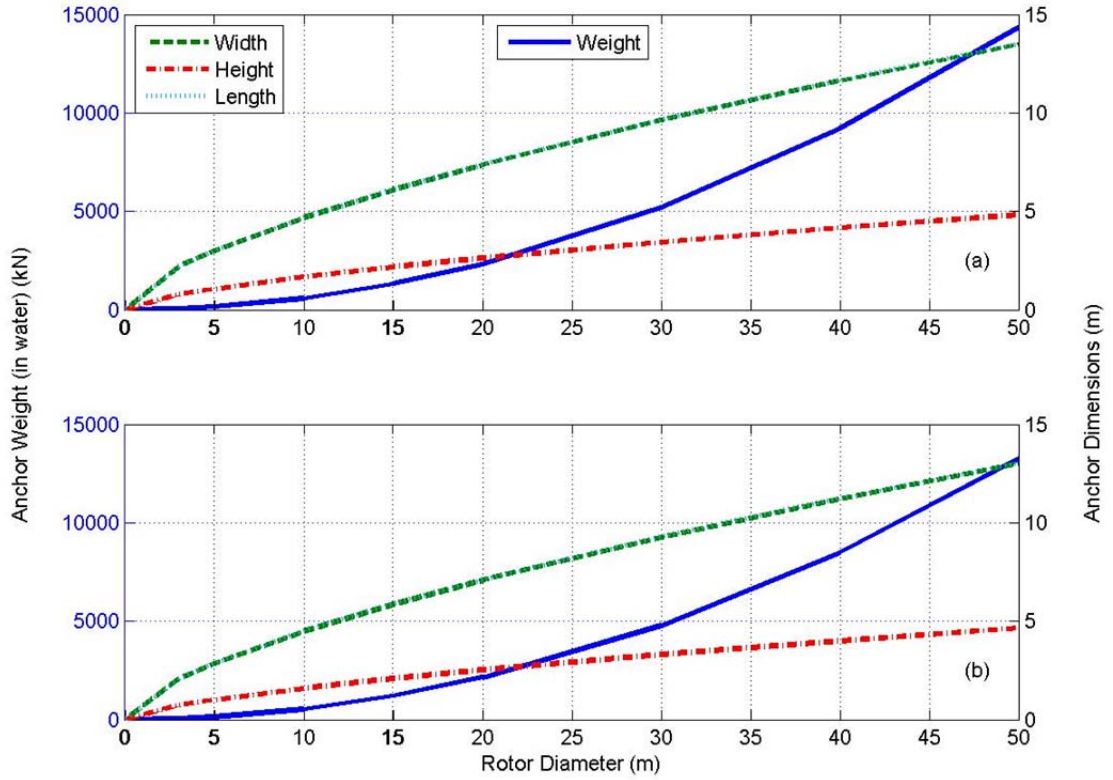
**Figure 14: Anchor dimensions for concrete deadweight anchor with no shear keys at 700 m depth location for loose sand with a friction angle of 30˚. Mooring scope of 1.25 (a) and 1.50 (b) are presented. Anchor length and width overlay each other in this figure.**

### 4.1.2 **Deadweight Anchor on Cohesive Soil with no Shear Keys**

Areas of sediment observed during past surveys may be cohesive depending on the soil's grain size distribution and its index properties such as water content (NCEL 1985). The holding capacity of a simple deadweight anchor in cohesive soil such as clay, silt, or mud was approximated by:

$$F_h = S_{uz}(A) + (2S_{ua}z + \frac{1}{2}\gamma_b z^2)B , \qquad (6)$$

where $S_{uz}$ is the un-drained shear strength at the bottom of the anchor, $A$ is the plan area, $S_{ua}$ is the average un-drained shear strength for depth $z$, $z$ is the depth from the

surface of the seabed to the bottom of the anchor, and $\gamma_b$ is the buoyant specific weight of soil (Sound and Sea Technology 2009). Shear strength can be measured at the deployment location or can be estimated for preliminary sizing using:

$$S_{uz} = \frac{W}{N_c A},$$ (7)

where $N_c$ is the bearing capacity factor, conservatively approximated at 5.7 by Sound and Sea Technology (2009). The average shear strength, if assumed to increase linearly from zero at the surface, is

$$S_{ua} = 0.5 S_{uz}$$ (8)

and the depth is

$$z = \frac{S_{uz}}{G_{su}},$$ (9)

where $G_{su}$ is the rate of increase of shear strength with depth, approximated at 1.89 kN/m$^3$ (12 psf/ft) (Sound and Sea Technology 2009). Using these estimates for cohesive soil properties, the horizontal loads $(F_h)$ obtained from the simulation, and the buoyant weight for soil of 4.4 kN/m$^3$ (28 pcf) suggested for clay by Taylor (1982), the equation for holding capacity only has two unknowns, weight and plan area,

$$F_h = \frac{W}{N_c} + \left[ \frac{\sqrt{A} W^2 (2G_{su} + \gamma_b)}{2A^2 N_c^2 G_{su}^2} \right].$$ (10)

To solve this equation, one dimension has to be assumed to size the other. The plan area was assumed to be square, so the width $(B)$ given in Equation 6 was replaced by the square root of the area $(A)$.

The design solution presented in this paper used the anchor plan areas from Section 4.1.1 in Equation 10 in to determine anchor weights (Figures 15 and 16). Alternatively, the anchor weights from Section 4.1.1 can be plugged into Equation 10 to determine the corresponding plan areas. These solutions can be found in (Seibert 2011). For both solutions, the heights of the anchors were determined from the volume of concrete necessary to create the required anchor weight in water. In the case of a 20 m diameter rotor at the 325 m location, there was a 2.77% increase in weight, 5.6% increase in plan area, and a 2.8% decrease in height when determining anchor dimensions from measured anchor weights instead of determining anchor weights from dimensions (Seibert 2011) as shown in this paper.
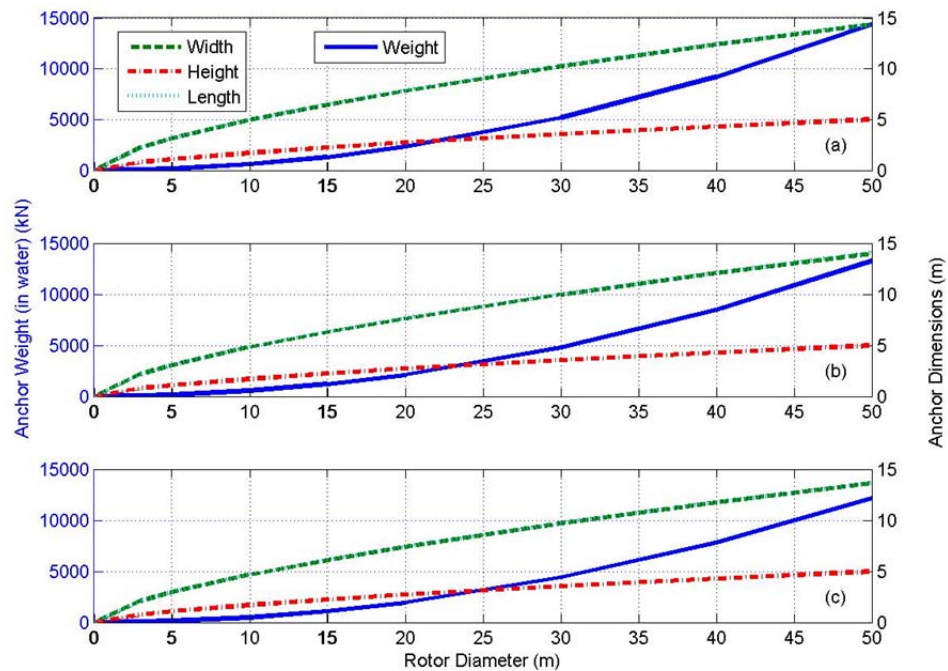


**Figure 15: Anchor dimensions for concrete deadweight anchor with no shear keys at 325 m depth location for cohesive soil using the plan area solved for in the previous section. Mooring scopes of 1.25 (a), 1.50 (b), and 2.0 (c) are presented. Anchor length and width overlay each other in this figure.**
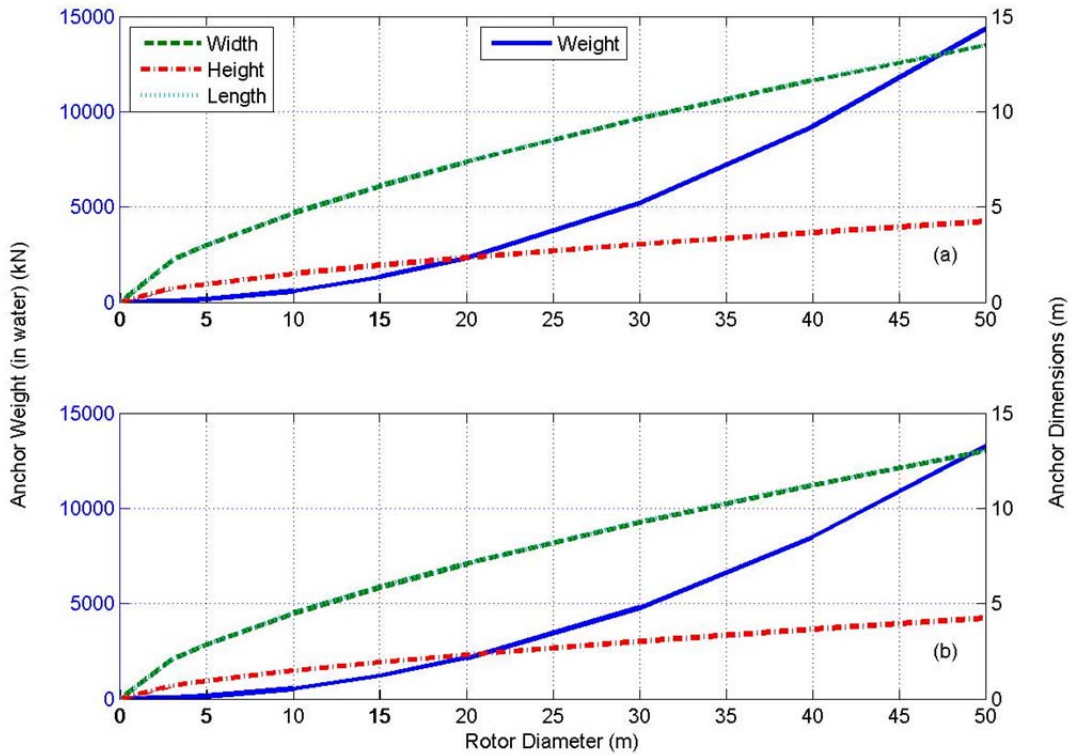
27

**Figure 16: Anchor dimensions for concrete deadweight anchor with no shear keys at 700 m depth location for cohesive soil using the plan area solved for in the previous section. Mooring scopes of 1.25 (a) and 1.50 (b) are presented. Anchor length and width overlay each other in this figure.**

### 4.1.3 **Deadweight Anchor on Cohesionless Soil with Shear Keys**

Shear keys increase lateral anchor holding capacity by inducing failure in the soil and not at the anchor soil interface (Taylor 2010). Precise deadweight anchor sizing and shear key design can be found with an iterative process to discover the weight necessary to resist sliding along with anchor width. A grid of shear keys can then be designed, but it must be ensured that the weight of the anchor will fully embed the shear keys. If this is not accomplished, either the anchor weight must be increased or shear keys redesigned. Although an iterative process is demonstrated in Taylor (1982) to design and size shear keys, a single formula can be used to determine preliminary anchor weight of a

28

deadweight anchor with full-base keying skirts. The lateral capacity of a deadweight anchor with full-base keying skirts in cohesionless soil was calculated as (Sound and Sea Technology 2009):

$$F_h = (W - F_v)(\tan \phi_s) + K_p \gamma_b \frac{1}{2} z_s^2 B ,$$
(11)

where $\tan \phi_s$ is the tangent of the friction angle at depth $z_s$, $z_s$ is depth to the bottom of the skirts, and $K_p$ is the passive earth pressure coefficient equal to:

$$K_p = \tan^2 (45 + \phi / 2) .$$
(12)

The tangent of friction angle at depth $z_s$ for the trapped soil was set as 0.67 (Sound and Sea Technology, 2009). The coefficient $\gamma_b$ for sand, with an angle of internal friction of 30°, was set at 8.63 kN/m$^3$ (55 pcf), and shear key penetration depth of $0.05B$ is assumed as a minimum (Taylor 1982).

Both anchor weight and width are unresolved variables in Equation 11. Therefore, the anchor widths determined in Section 4.1.1 were used, and the anchor weight with shear keys is calculated. Figure 17 shows the necessary anchor weight for increasing rotor diameters at each location. For a 20 m diameter rotor blade at the 325 m location with a scope of 1.25, the necessary submerged anchor weight was reduced from 2,312.8 kN without shear keys to 1,720.0 kN with shear keys, a 25.6% reduction.
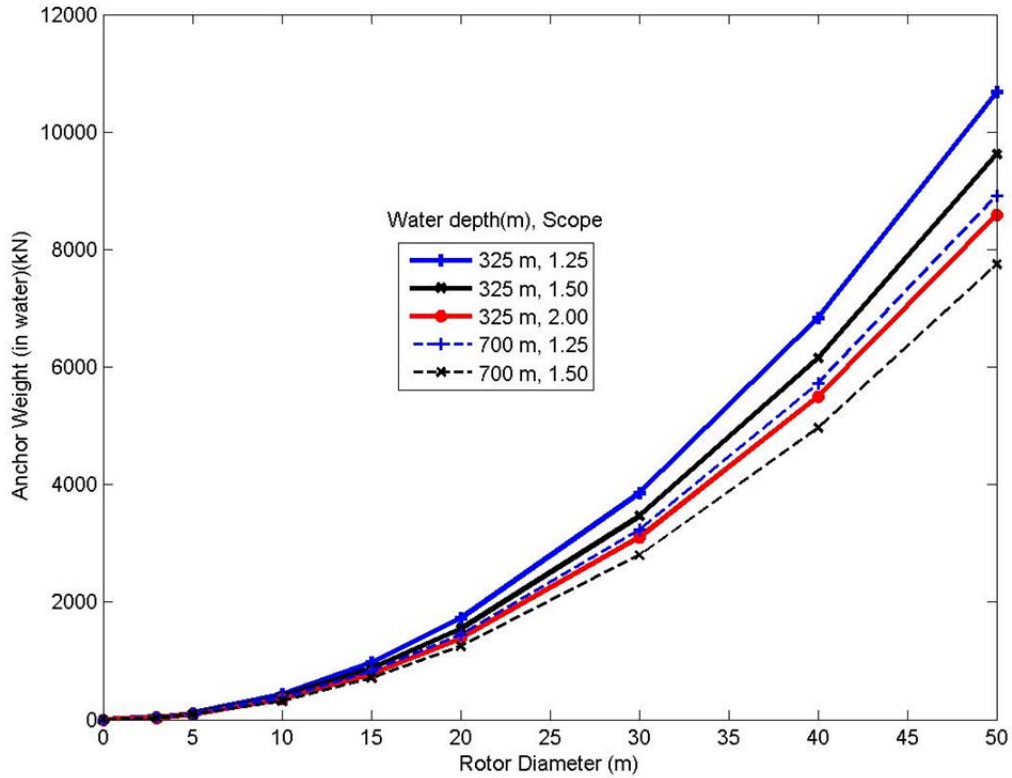
**Figure 17: Necessary anchor weight of concrete deadweight with full keying skirts on cohesionless soil at each location.**

### 4.1.4  **Deadweight Anchor with Shear Keys on Cohesive Soil**

Solving for the necessary submerged weight of a deadweight anchor with shear keys on cohesive soil has been addressed with set dimension ratios by Taylor (1982). The necessary submerged weight to resist overturning a deadweight anchor with shear keys on cohesive soil, for an anchor height of $H = 0.2B$ and a shear key penetration of $z_s = 0.1B$, is calculated by:

$$W=1.2F_h + F_v, \tag{13}$$

where $F_h$ is the horizontal anchor loading and $F_v$ is the vertical anchor loading (Taylor, 1982). When designing the anchor, it is required that the submerged weight solved using

Equation 13 is larger than the weight required to embed the shear keys. If not, a larger weight must be selected or shear keys must be redesigned to assure penetration. For a 20 m diameter rotor blade at the 325 m location with a mooring scope of 1.25, the necessary anchor weight was reduced from 2,250.5 kN (Figure 15) to 1,588.0 kN (Figure 18) with shear keys, a 29.4% reduction. Detailed shear key design methods can be completed for each case using methods presented in *Interaction of Anchors with Soil and Anchor Design* (Taylor 1982).
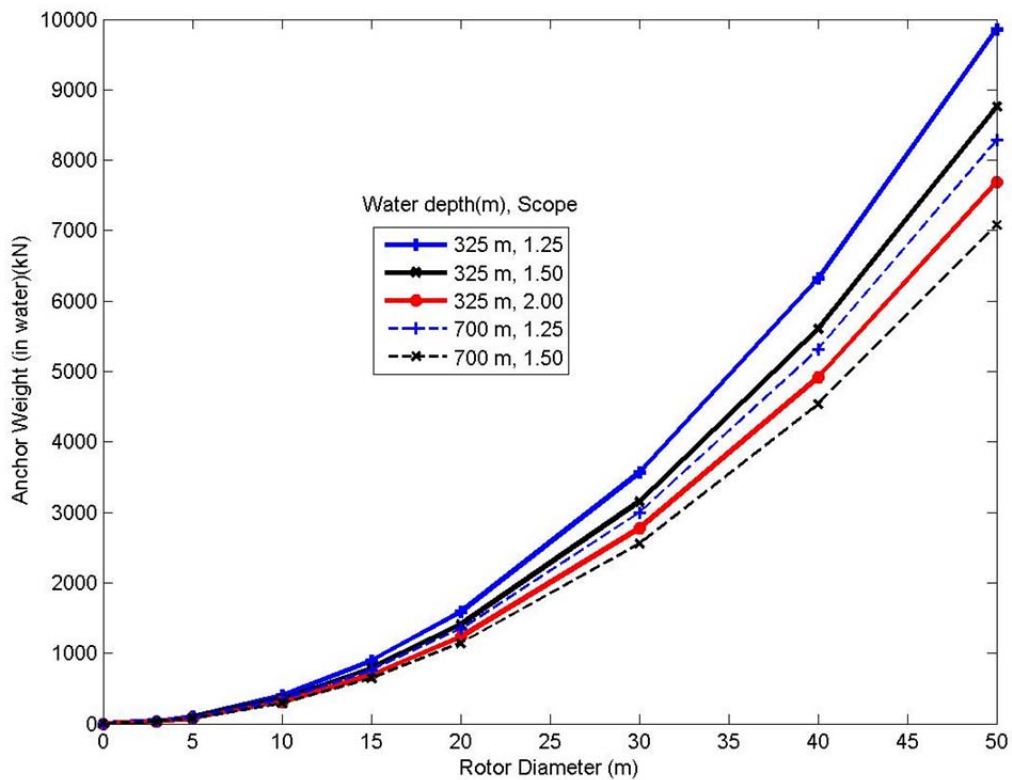


**Figure 18: Necessary weight of deadweight anchor with shear keys to resist overturning in cohesive soil.**

## 4.2   Driven Plate Anchors

Pile-driven plate anchors function by being forced into the seafloor by a pile-driving

hammer to what is referred to as the "driven depth" (Forrest et al. 1995). The follower, which is a structural component attached to a plate while being driven by the hammer, is retrieved, and the anchor is pull-tested to rotate, or "key" the anchor into its operating position, the "keyed depth" (Forrest et al. 1995).

### 4.2.1 **Driven Plate Anchors in Cohesionless Soil**

The holding strength of driven plate anchors in cohesionless soil is directly related to the keyed depth of the anchor. It is also dependent on the size of the plate and the strength of the soil (Forrest et al. 1995). The necessary keyed depth of driven plate anchors in cohesionless soil was found using:

$$D = \frac{F_u}{A g_b N_q},$$
(16)

where $F_u$ is the ultimate anchor holding capacity, $A$ is the area of the plate, $g_b$ is the effective (buoyant) weight of the soil, $D$ is the embedded depth of the (keyed) anchor, and $N_q$ is the holding capacity factor for cohesionless soils (Forrest et al. 1995). For a primarily horizontal anchor loading, the ultimate anchor capacity can be increased by a factor of 1.25 to account for the embedded chain (Forrest et al. 1995). No safety factors were applied to the anchor sizing, although it is recommended to apply a safety factor of 2 for most applications (Forrest et al. 1995). Areas of the driven plates evaluated in this section range from 1 to 4 m$^2$ at increments of 0.5 m$^2$. The effective (buoyant) weight for sand ($g_b$) with a friction angle of 30° is 7.85 kN/m$^3$ (50 pcf) (Forrest et al. 1995). This value for the buoyant weight of sand (with a friction angle of 30˚) is 0.78 kN/m$^3$ less than the value presented in Section 4.1.3. To resolve this conflict, the corresponding value

32

suggested by the source of the accompanying equation was selected.

The holding capacity factor ($N_q$) was selected from curves presented in Forrest et al. (1995) for a friction angle of 30°. This reference suggests a holding capacity factor of more than 10 for an embedment depth to anchor width ratio greater than 6. A holding capacity of 10 was conservatively chosen, although in both normally consolidated soils or over-consolidated clay, if the keyed depth to width ratio ($D/B$) is 6 or greater, long term load capacity factors in excess of 15 are noted (Forrest et al. 1995).

The necessary keyed depths are displayed in Figures 19 and 20 based on the assumptions and selections outlined above. The associated anchor driven depth can be determined with methods presented in *Design Guide for Pile Driven Plate Anchors* to ensure the final anchor position is at the necessary keyed depth.
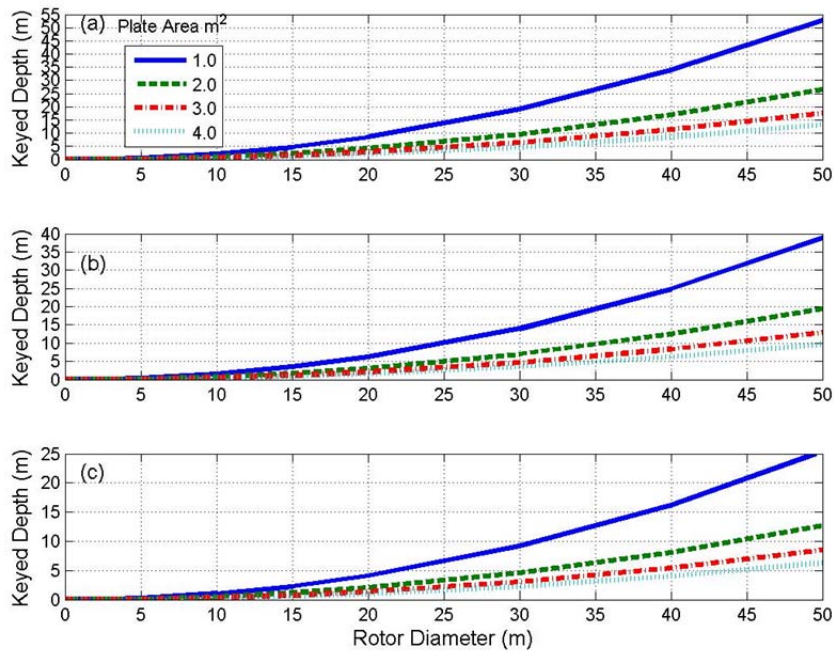


**Figure 19: Necessary keyed depth for seven plate areas presented as a function of rotor diameter at 325 m depth location for loose sand. Mooring scopes of 1.25 (a), 1.50 (b), and 2.00 (c) are presented.**
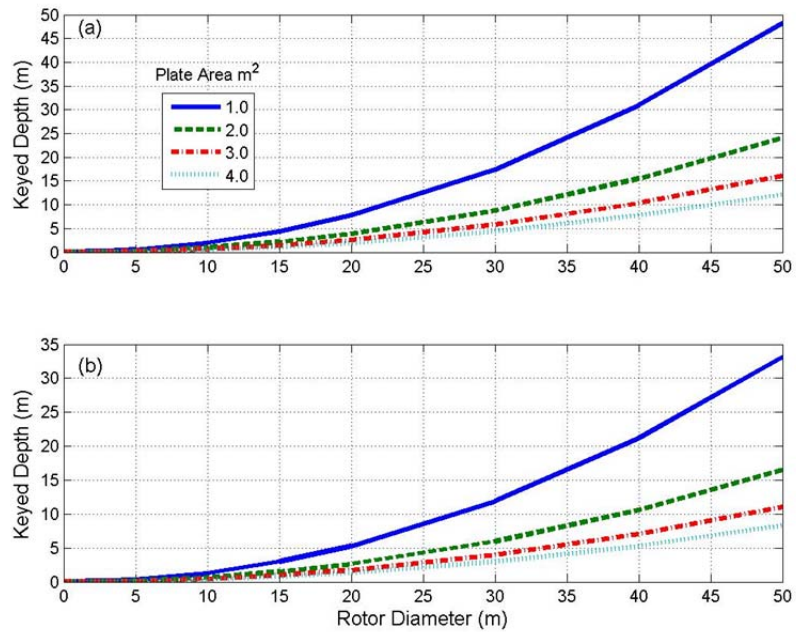
33

**Figure 20: Necessary keyed depth for seven plate areas presented as a function of rotor diameter at 700 m depth location for loose sand. Mooring scopes of 1.25 (a) and 1.5 (b) are presented.**

### 4.2.2 Driven Plate Anchors in Cohesive Soil

Similar to driven plates in cohesionless soil, plate anchor holding capacity in cohesive soil is directly related to plate size and soil strength. The necessary plate area $(A)$ for varying cohesive soil shear strengths (c) is determined using:

$$A = \frac{F_u}{cN_c}, \tag{14}$$

where $F_u$ is the ultimate anchor holding capacity and $N_c$ is the bearing capacity factor for cohesive soils (Forrest et al. 1995). A maximum $N_c$ of 12 is recommended for all marine (saturated) installations by (Forrest et al. 1995). Using this capacity factor and the soil shear strength, the required plate anchor size can be calculated from Equation 14. Using a soil shear strength of 22 kPa, a value that is within the ranges suggested for "soft

34

clay" by both American (ASTM D-2488) and British (BS CP-2004) standards (Vryhof Anchors 2005), a turbine with a 20 m rotor and 1.25 mooring scope will require a plate anchor area of 2.6 $m^2$. This same loading scenario will require a 0.55 $m^2$ plate anchor when using a soil shear strength of 100 kPa, a value that is within the ranges suggested for "firm clay" by both American (ASTM D-2488) and British (BS CP-2004) standards (Vryhof Anchors 2005). For the same mooring scenarios and soil shear strengths, a turbine with a 50 m diameter rotor will require plate anchor area greater than 9 $m^2$ for soft clay (a size that is likely un-feasible) and 3.5 $m^2$ for firm clay. The required embedment depths can then be determined based upon the soil properties following Forrest et al. (1995), with embedment depth versus anchor diameter ratio ranging from 1.7 to 4.3. To achieve the assumed holding capacity factor of 12, the embedment depth-to-diameter ratios should exceed 4.0 for a soil shear strength of 22 kPa and 4.3 for a soil shear strength of 100 kPa (according to Figure 3-5 presented by Forrest et al. 1995).

## 4.3   Traditional Drag Embedment Anchors

Traditional drag embedment anchors are not suitable for the proposed anchor loading scenarios because of high uplift angles of taut moorings. Instead, drag embedment anchors are typically selected for catenary moorings, which could be used for select MRE anchor systems. Since it is difficult to predict the holding capacity of a drag embedment anchor, estimates are normally obtained through empirical means. True holding capability can only be determined after deployment (API 2005). Estimates for horizontal anchor holding capacity based on Navy Techdata Sheets, industry anchor tests, and field experience can be found for sand and soft clay or mud in (API 2005). Conversely, anchor

guidelines for predicting holding capacity in hard clay, calcareous sand, coral, rock seafloor or layered floors were not available at the time that API RP2SK was written (API 2005).

Catenary moorings typically include lengths of chain on the seafloor to convert vertical loads to lateral loads. However, mooring scopes can also be reduced by adding a clump weight to the mooring configuration to negate vertical loading on the drag embedment anchor. Additional holding capacity from chain and wire rope on the seafloor can be predicted with methods found in API RP2SK.

The horizontal anchor loadings presented in Figures 10 and 11 differ by less than 5% for their respective locations. This is because the majority of lateral anchor loading is from the horizontal drag of the rotor and not the increase in line length. An estimate of the size and type of traditional embedment anchor that could resist the horizontal loading induced by a 50 m diameter rotor turbine can be determined by assuming that horizontal anchor loading is not a function of scope and uplift angle is 0°. The maximum horizontal anchor loading for a 50 m diameter rotor is 4760 kN (1070 kips) at the 325 m depth location. This is the maximum horizontal load of all simulations conducted, and would require an anchor size of 177.9 kN (40 kips) for Boss and Navmoor anchors, or a 444.8 kN (100 kips) Stevin anchor for a sand bottom. Soft clay or mud bottom composition requires a 213.5 kN (48 kips) Bruce FFTS MK III or Stevpris MK III. Alternatively, a 444.8 kN (100 kips) Moorfast or Offdrill II anchor can be used. These estimates do not take into account the decrease in horizontal anchor loading due to friction of chain on the seafloor, nor were there safety factors applied.

While traditional drag embedment anchors are not applicable to taut moorings, there is a design available for use with taut moorings. Vertical loaded anchors (VLA), such as the Vryhof Stevmanta VLA, are suitable for use in soft clay soil conditions and are embedded into the seabed like a conventional drag embedment anchor (Ruinen n.d.). Upon adjusting the anchor into normal mode with either the use of two mooring lines or a shear pin, it can resist high uplift angles (Ruinen n.d.). This anchor design is an option for MRE devices where high uplift capacity can be obtained by deep penetration into soft soil (Ruinen n.d.).

## 4.4  Pile Anchors

Pile anchors are typically used as a final option when less costly anchors, like those described earlier, are not sufficient. Drilled and grouted piles might also be a desirable anchoring method in rock seafloors if a footprint smaller than those created by large gravity anchors are desired. Increased costs are associated with significant floating assets required for transportation, installation support, and obtaining geophysical and geotechnical data required for penetration depths reaching tens of meters (Sound and Sea Technology 2009). However, is stated in the OWET studies that, "piles may afford an economical mooring solution for large scale commercial WEC system installations" (Sound and Sea Technology 2009). This option may also be an economical mooring solution for large scale commercial OCT deployments. Performing generalized preliminary sizing of piles without specific site conditions is difficult because designing piles requires the most comprehensive geotechnical data of all anchor types (Sound and Sea Technology 2009). Also, variations in pile design make it difficult to present

generalized preliminary sizing for pile anchor types.

If the approximate maximum capacities presented by Sound and Sea Technology (2009) are used for anchor capacity estimates, an estimate to the maximum rotor diameter applicable to each type of pile anchor can be determined. For pile and H-pipe anchors, approximated maximum capacities for both axial and lateral loading are greater than the estimated vertical and horizontal loading of all MHK mooring scenarios presented in Section 3.3.1. The calculated anchor loadings and the capacities of umbrella piles and chain-in-hole piles are presented together in Figure 21. These results suggest that, for a 1.25 scope (and the evaluated loading scenario in a 325 m water depth), an umbrella pile is suitable for rotor diameters up to 13 m in mud and 23 m in sand, while chain-in-hole pile can be used for rotor diameters up to 31 m.

More detailed anchor design may reveal pile anchors have a larger capacity because lateral capacity can be increased by methods such as lowering the mooring line attachment point, burying the pile below grade, attaching fins to the upper end of the pile, or using an upper-end shear collar and lower-end anchor to effect a combination of increased soil bearing and confinement with uplift resistance (Sound and Sea Technology 2009). The method of combining multiple piles into cluster piles is also an option where increased loading capacity is required.
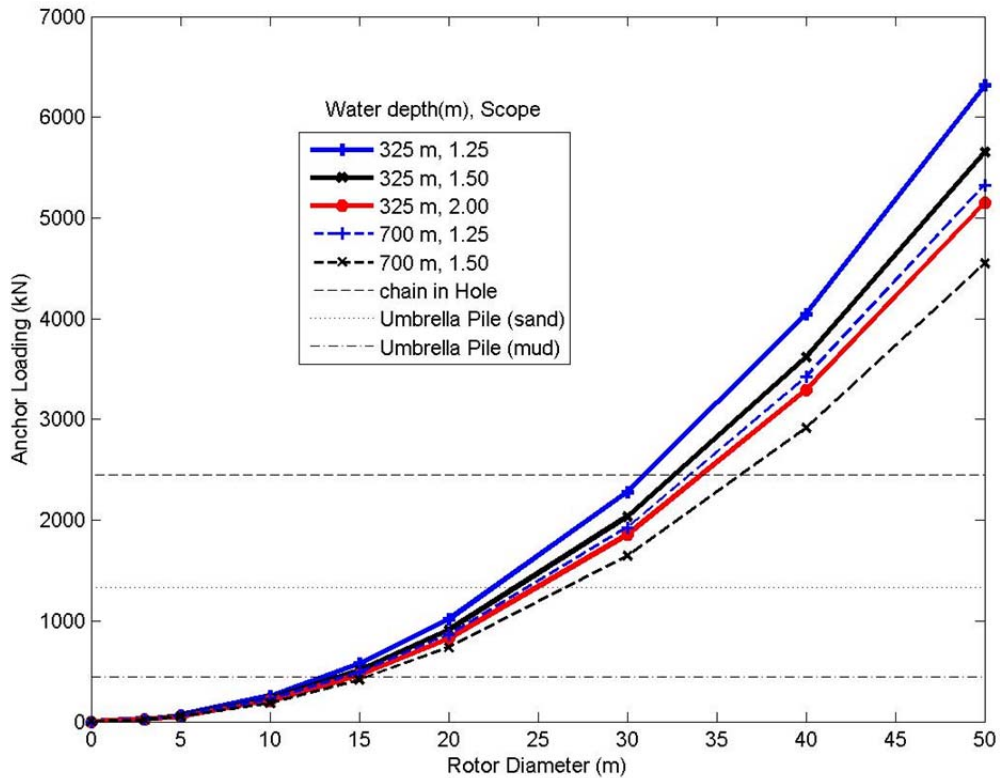
**Figure 21: Turbine Anchor Loading plotted along with Approximate Maximum Capacities of Pile Anchors.**

## 5. Conclusions

An anchor study is presented in this paper for an area off of the coast of Southeast Florida that is being considered for commercial marine renewable energy extraction. Applicable OCT devices were discussed, and an examination of the potential anchoring systems that could be used to hold these systems in place for local environmental conditions was presented.

This study included a regional review of bottom types based on the existing benthic survey data. These surveys revealed areas with minimal slope and low relief west of the Miami Terrace Escarpment in approximately 200 to 400 m water depth and east of the Miami Terrace Escarpment in approximately 600 to 800 m water depth, which may be

suitable locations for OCT system anchoring. West of the Miami Terrace Escarpment, hard limestone bottoms, gravel or rubble bottoms, and hard bottoms overlaid by sand (stratified seafloors) were observed that will limit suitable anchor types to either deadweight or pile anchors. However, some smaller areas of sediment were also observed atop of the Miami Terrace, and if adequate sediment depths exist in these locations, all examined anchor types could be used. In areas east of the Miami Terrace Escarpment, where a mostly sediment bottom was observed, all four examined anchor types will function desirably if required sediment depths exist for respective types of anchors. Although anchoring may be possible on areas of the Miami Terrace Escarpment that combine steep slopes and high relief (being mindful of likely increased cost and uncertain performance), it may be possible to avoid these risks if more efficient and reliable anchoring can be achieved in locations to the west and east.

Anchor loading predictions were extracted from numerical simulations of moored OCTs with environmental conditions characteristic of the region of proposed deployment. Results from these simulations were used to size anchors applicable to taut mooring systems. Deadweight anchors with and without shear keys in cohesionless and cohesive soils were sized. These results were also applied to sizing driven plate anchors in cohesionless and cohesive soils. Traditional drag embedment anchors were evaluated with OCT simulation results as well. However, because of traditional limitations of these systems, a catenary mooring was assumed. Finally, estimated maximum capacities of pile anchors were overlaid on the anchor loading plots to identify maximum rotor diameters associated with each pile anchor type.

## ACKNOWLEDGMENTS

## REFERENCES

American Petroleum Institute (API) (2005). *Design and analysis of stationkeeping systems for floating structures*, Third Ed., API RP 2SK.

Ballard, R., and Uchupi, E. (1971). "Geological observations of the Miami Terrace from the submersible Ben Franklin." *J. Marine Tech. Soc.*, 5, 43-48.

Clarke, J., Grant, A., Connor, G., and Johnstone, C. (2009). "Development and in-sea performance testing of a single point mooring supported contra-rotating tidal turbine." *Proc. Int. Conf. on Ocean, Offshore, and Arctic Eng.*, Honolulu, HI, May 31 – June 5, OMAE2009-79995

Davis, B. V., Farrell, J. R., Swan, D. H., and Jeffers, K. A. (1986). "Generation of electric power from the Florida Current." *Proc. 18th Offshore Technology Conference,* Houston, TX, May 5-8, OTC-5120.

Driscoll, F. R., Skemp, S. H., Alsenas, G. M., Coley, C. J., and Leland, A. (2008). "Florida's Center for Ocean Energy Technology." *Proc. MTS/IEEE Oceans Conference*, Quebec City, Canada, Sept. 15-18, Oceans.2008.5152102

Duerr, A. E. S., and Dhanak, M. R. (2010). "Hydrokinetic power resource assessment of the Florida Current." *Proc. MTS/IEEE Oceans Conference*, Seattle, WA, Sept. 20-23, Oceans.2010.5664377

Forrest, J., Taylor, R., and Bowman, L. (1995). "Design guide for pile driven plate anchors." *Technical Rep.: TR-2039-OCN*, Naval Facilities Eng. Service Center, Port Hueneme, CA.

Leland, A. (2009). "A resource assessment of Southeast Florida as related to ocean thermal energy." MS Thesis, Florida Atlantic University, Boca Raton, FL.

Messing, C. G., Walker, B. K., Dodge, R. E., Reed, J., and Brooke, S. D. (2006.a). "Calypso LNG Deepwater Port Project, Florida marine benthic video survey." *Technical Rep.:* to Ecology and Environment, Inc. & SUEZ Energy North America, Inc.

Messing, C. G., Walker, B. K., Dodge, R. E., and Reed, J. (2006.b). "Calypso U.S. Pipeline, LLC, Mile Post (MP) 31- MP 0 Deep-water marine benthic video survey." *Technical Rep.:* to Calypso U.S. Pipeline, LLC.

NDBC - Moored Buoy Program. National Data Buoy Center. NOAA. (2010). Available: http://www.ndbc.noaa.gov/mooredbuoy.shtml, Accessed April 25.

National Civil Engineering Laboratory (NCEL) (1985). *Handbook for Marine Geotechnical Engineering.* Port Hueneme, CA.

Neumann, A. C., and Ball, M. M. (1970). "Submersible observations in the Straits of
    Florida: geology and bottom currents." *Geol. Soc. Amer. Bull.*, 81, 2861-2874.

Raye, R. E. (2002). "Characterization study of the Florida Current at 26.11 north latitude,
    79.50 west longitude for ocean current power generation." MS Thesis, Florida
    Atlantic University, Boca Raton, FL.

Ruinen, R. (n.d.). "Use of drag embedment anchor for floating wind wurbines." Pres. by
    Vryhof Anchors BV.

Seelig, W. N., Taylor, R., and Bang, S. (2001). "Improved Pearl Harbor and Kings Bay
    anchor designs." *Technical Rep.: TR-6073-OCN*, Naval Facilities Engineering
    Service Center, Port Hueneme, CA.

Seibert, M. G. (2011). "Determining anchoring systems for marine renewable energy
    devices moored in a western boundary current." MS Thesis, Florida Atlantic
    University, Boca Raton, FL.

SNMREC (2010). "NOEL Phase 1a – Temporary ocean current observing and
    monitoring system." Dania Beach, FL. Unpublished.

Sound and Sea Technology (2009). "Advance anchoring and mooring study." *Technical
    Rep.:* for Oregon Wave Energy Trust.

Taylor, R. J. (1982). "Interaction of anchors with soil and anchor design." Naval Civil
    Engineering Laboratory. Port Hueneme, CA.

Taylor, R. J. (2010). Email: October 19, 2010.

Deep Water Moorings. (2010). Available:
    http://www.tensiontech.com/services/mooring.html, Accessed: November 27

VanZwieten, J., Driscoll, F. R., Leonessa, A., and Deane, G. (2006.a). "Design of a prototype ocean current turbine—Part I: mathematical modeling and dynamics simulation." *Ocean Eng.*, 33(11-12), 1485-1521

VanZwieten, J., Driscoll, F. R., Leonessa, A., and Deane, G. (2006.b). "Design of a prototype ocean current turbine—Part II: flight control system." *Ocean Eng.*, 33(11-12), 1522-1551

VanZwieten, J. H., Vanrietvelde, N., and Hacker, B. (2010). "Numerical simulation of an experimental ocean current turbine." Submitted to *J. Oceanic Eng.*, 2010JOE000780.

VanZwieten, J. H., Oster, C. M., and Duerr, A. E. S. (2011). "Design and analysis of a rotor blade optimized for extracting energy from the Florida Current." *Proc. Int. Conference on Ocean, Offshore, and Arctic Eng.*, Rotterdam, Netherlands, June 19-24, OMAE2011-49827.

Vryhof Anchors (2005). *Anchor Manual 2005.* Krimpen a/d yssel, Netherlands.